

# Nitrogen flux into metabolites and microcystins changes in response to different nitrogen sources in *Microcystis aeruginosa* NIES-843

Lauren E. Krausfeldt<sup>1</sup> Abigail T. Farmer,<sup>2</sup>  
Hector F. Castro,<sup>2</sup> Gregory L. Boyer,<sup>3</sup>  
Shawn R. Campagna<sup>2</sup> and Steven W. Wilhelm<sup>1\*</sup>

<sup>1</sup>Department of Microbiology, University of Tennessee, Knoxville, TN.

<sup>2</sup>Department of Chemistry, University of Tennessee, Knoxville, TN.

<sup>3</sup>Department of Chemistry, State University of New York, College of Environmental Science and Forestry, Syracuse, NY.

## Summary

The over-enrichment of nitrogen (N) in the environment has contributed to severe and recurring harmful cyanobacterial blooms, especially by the non-N<sub>2</sub>-fixing *Microcystis* spp. N chemical speciation influences cyanobacterial growth, persistence and the production of the hepatotoxin microcystin, but the physiological mechanisms to explain these observations remain unresolved. Stable-labelled isotopes and metabolomics were employed to address the influence of nitrate, ammonium, and urea on cellular physiology and production of microcystins in *Microcystis aeruginosa* NIES-843. Global metabolic changes were driven by both N speciation and diel cycling. Tracing <sup>15</sup>N-labelled nitrate, ammonium, and urea through the metabolome revealed N uptake, regardless of species, was linked to C assimilation. The production of amino acids, like arginine, and other N-rich compounds corresponded with greater turnover of microcystins in cells grown on urea compared to nitrate and ammonium. However, <sup>15</sup>N was incorporated into microcystins from all N sources. The differences in N flux were attributed to the energetic efficiency of growth on each N source. While N in general plays an important role in sustaining biomass, these data show that N-speciation induces

physiological changes that culminate in differences in global metabolism, cellular microcystin quotas and congener composition.

## Introduction

Increasing nitrogen (N) inputs into the environment due to agricultural and industrial processes have corresponded to the global expansion of toxic cyanobacterial blooms, especially those caused by the non-N<sub>2</sub>-fixing *Microcystis* spp. that are often dominant bloom formers in lakes. N-enrichment in these ecosystems, especially in combination with phosphorus (P)-loading, contributes to bloom formation and persistence, severely impacting water quality and posing severe risks to aquatic life and human health (Paerl *et al.*, 2014). While it is likely that in many cases the availability of P might constrain the biomass of primary producers in fresh waters (Schindler, 1977; Schindler and Vallentyne, 2008), it is equally likely that the concentration and chemistry of nitrogenous chemicals shapes biomass as well as the diversity of the plankton community that is present (Wilhelm *et al.*, 2003; Paerl *et al.*, 2016). N-enrichment has also been linked to the production of cyanotoxins, such as the microcystins (MCs), produced by several *Microcystis* spp. and other bloom-forming cyanobacteria (Davis *et al.*, 2010; Gobler *et al.*, 2016; Hampel *et al.*, 2019; Newell *et al.*, 2019). The specific role of N in toxicity of blooms remains uncertain, likely in large part due to the incomplete understanding of the general function and regulation of MCs in cyanobacterial cells on a physiological level (Neilan *et al.*, 2013; Bullerjahn *et al.*, 2016). MC concentrations have been reported to increase in response to N-loading in the field (Harke and Gobler, 2015; Gobler *et al.*, 2016). This may be a result of a selection for MC producers over non-producers due to N enrichment, as not all *Microcystis* spp. have the genetic potential for MC production. Alternatively, N-enrichment could be causing *Microcystis* capable of producing MCs to increase their production. Being comprised of seven amino acids (Carmichael and Boyer, 2016), MCs are N-rich, suggesting N availability plays a role to some extent in the production of MCs in

Received 28 January, 2020; revised 13 April, 2020; accepted 18 April, 2020. \*For correspondence. E-mail wilhelm@utk.edu; Tel. 865-974-0665; Fax 865-974-4007.

© 2020 Society for Applied Microbiology and John Wiley & Sons Ltd.

nature. However, on a cellular level, the effect of N availability or speciation on the production of cyanotoxins is not yet clear (Ginn *et al.*, 2010; Harke *et al.*, 2015; Gobler *et al.*, 2016; Peng *et al.*, 2018).

N availability and speciation play important roles in microbial community dynamics, and this is a critical consideration when predicting the severity or toxicity of *Microcystis* blooms. *Microcystis* can use both inorganic N, like nitrate ( $\text{NO}_3^-$ ) and ammonium ( $\text{NH}_4^+$ ), and organic forms, like amino acids and urea (Steffen *et al.*, 2014; Erratt *et al.*, 2018; Peng *et al.*, 2018). Inorganic N sources are often the focus of studies investigating the link between N enrichment, MCs, and the dominance of toxin producing species. However, with the switch to the organic N fertilizer, urea, in agricultural practices over the past few decades (Paerl *et al.*, 2016), the role of urea has been proposed as a contributing factor (Glibert *et al.*, 2006; Glibert *et al.*, 2014; Belisle *et al.*, 2016). Urea is commonly found in fresh waters that experience cyanobacterial blooms and are influenced by agriculture (Glibert *et al.*, 2014; Belisle *et al.*, 2016). In culture experiments, growth rates, photosynthetic health, concentrations of MCs, and composition of total MCs and congeners are altered when cells are grown on different N species (Erratt *et al.*, 2018; Peng *et al.*, 2018), and several field studies have supported this (Davis *et al.*, 2010; Chaffin and Bridgeman, 2013; Beversdorf *et al.*, 2015; Chaffin *et al.*, 2018). At times, results from these studies are seemingly contradictory, likely due to confounding factors regulating nutrient utilization, such as light, temperature, pH, and competition with heterotrophs. The physiological mechanisms to explain these observations are not clear but remain a crucial step in order to be linked to broader ecological implications.

The goal of this study was to examine the physiological response by *M. aeruginosa*, a model toxic *Microcystis* spp., to differences in N speciation by proxy of metabolic flux. Using  $^{15}\text{N}$ -labelled isotopes of  $\text{NH}_4^+$ , urea, and  $\text{NO}_3^-$ , N was traced through the metabolism of axenically grown *M. aeruginosa* in a manner akin to recent efforts to trace the fate of carbon from urea (Krausfeldt *et al.*, 2019). Specific cellular responses to these N species were identified and linked to differences in MC composition.

## Results

### Growth dynamics and metabolic trends

Axenic *M. aeruginosa* NIES-843 cells acclimated to  $\text{NO}_3^-$ ,  $\text{NH}_4^+$ , and urea as the sole N sources had an average doubling time during log phase of 2.19 ( $\pm 0.06$ ), 2.12 ( $\pm 0.35$ ), and 1.91 ( $\pm 0.29$ ) days, respectively, after  $^{15}\text{N}$  additions (Supporting Information Table S1). Differences in doubling times over 48 h were not significant (one-way

ANOVA,  $P = 0.3$ , Fig. 1A). A lag phase was observed in cell concentration used to estimate growth on urea in the first 24 h but reached the same cell concentration and maintained a similar maximum doubling time compared to the other N treatments over the 48 h period. Trends in fluorescence [fluorescent units (FSU)] of cultures grown on urea were comparable to other N treatments (Fig. 1B). Cells grown on  $\text{NH}_4^+$  had lower FSU values through the entire experiment, and by the second light cycle, the FSU in cultures grown on  $\text{NO}_3^-$  surpassed cultures grown on urea. Samples clustered by N treatment (ANOSIM,  $R = 0.803$ ,  $P = 0.001$ ) and light and dark cycles (ANOSIM,  $R = 0.518$ ,  $P = 0.001$ ; Fig. 1C). Samples collected during the dark cycle were different across N treatment (ANOSIM,  $R = 0.878$ ,  $P = 0.001$ ), and the same was observed for the samples collected during the light cycle (ANOSIM,  $R = 0.598$ ,  $P = 0.001$ ).

The influence of diel cycling on global metabolic profiles corresponded to differences in the dynamics between glutamate (GLU) and glutamine (GLN). Glutamate to glutamine ratios (GLU:GLN) can be indicative of the N status within the cell, with increased ratios indicating a cell is more N starved and decreased ratios indicating the cell's N demands have been met (Flynn *et al.*, 1989). GLU:GLN did not differ significantly ( $P = 0.56$ ) at  $T_0$  and showed similar trends across time on all N species. They decreased during the light cycle (cellular N became more replete) and increased during the dark cycle (cellular N became more deplete; Fig. 2A–C, Supporting Information Table S2). This was the most pronounced in cells grown on  $\text{NH}_4^+$ . Despite similarities in these trends, the trends in GLU and GLN abundances differed across N species (Supporting Information Fig. S1 and Table S4). Abundances of GLU and GLN increased on N species within the first 12 h. Fluctuations in GLU and GLN varied over time and differed across N treatment, with only GLN on  $\text{NH}_4^+$  and GLU on  $\text{NO}_3^-$  following a clear diel pattern (Supporting Information Table S3).

### $^{15}\text{N}$ labeling of the metabolome

Most metabolites detected with  $^{15}\text{N}$  in the 48 h experiment were labelled by  $T_6$  in cultures grown on all N species. All of the GLN and about 80% of the GLU was labelled with at least one  $^{15}\text{N}$  by  $T_6$  (Fig. 2D–F). Both GLU and GLN remained labelled in a consistent trend throughout the experiment (Fig. 2D and E, Supporting Information Fig. S2A–C). Trends in  $^{15}\text{N}$  labelling into GLU and GLN differed on  $\text{NO}_3^-$ , and it took until  $T_{48}$  for GLN and GLU pools to match labelled pools in  $\text{NH}_4^+$  and urea. Although the incorporation trends into the GLU and GLN pools were similar in cultures grown on  $\text{NH}_4^+$  and urea,  $\text{NH}_4^+$  had the highest proportion of GLN molecules

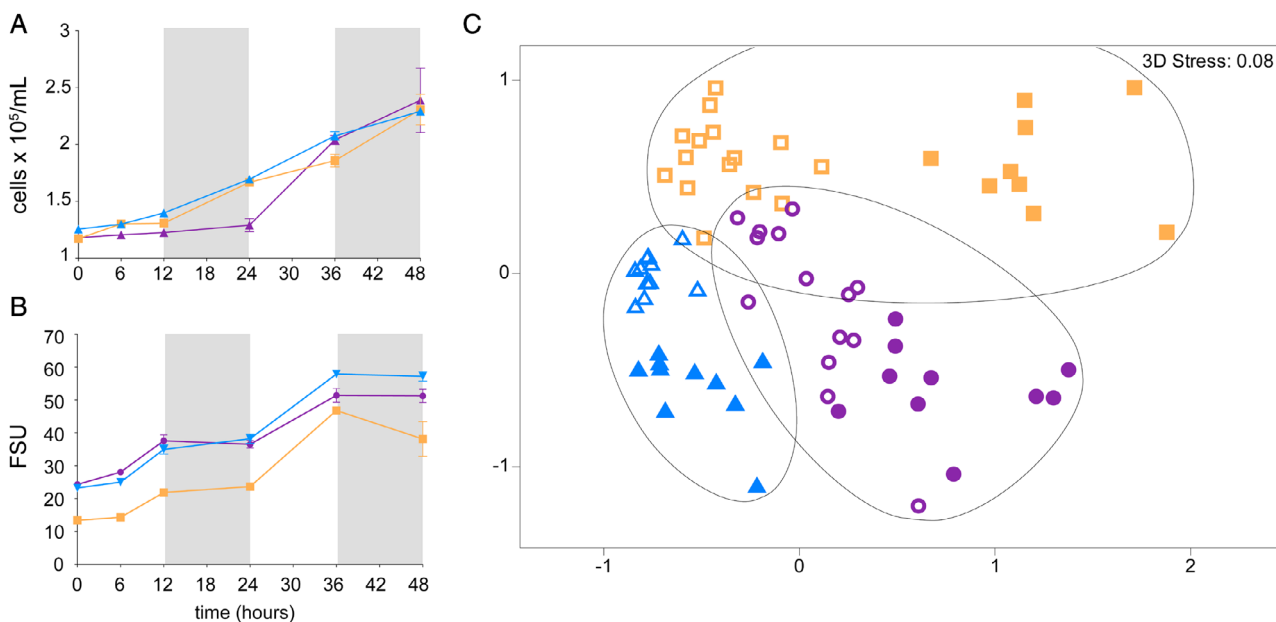


**Fig. 1.** Trends in growth and global metabolic profiles for each N treatment. A. Growth of *M. aeruginosa* before ( $T_0$ ) and after  $^{15}\text{N}$  additions is shown in cell number and (B) fluorescence (FSU). Shading represents time points that were collected during the dark cycle. C. Non-metric multidimensional scaling (NMDS) analysis showing relationships between samples based on treatment and time. Open symbols represent samples collected during the light cycle ( $T_0$ – $T_{12}$ ,  $T_{36}$ ) and closed symbols are samples collected during the dark cycle ( $T_{24}$ ,  $T_{48}$ ). Colours and shapes represent N treatment; blue triangles =  $\text{NO}_3$ , orange squares =  $\text{NH}_4$ , purple circles = urea. Error bars represent standard error.

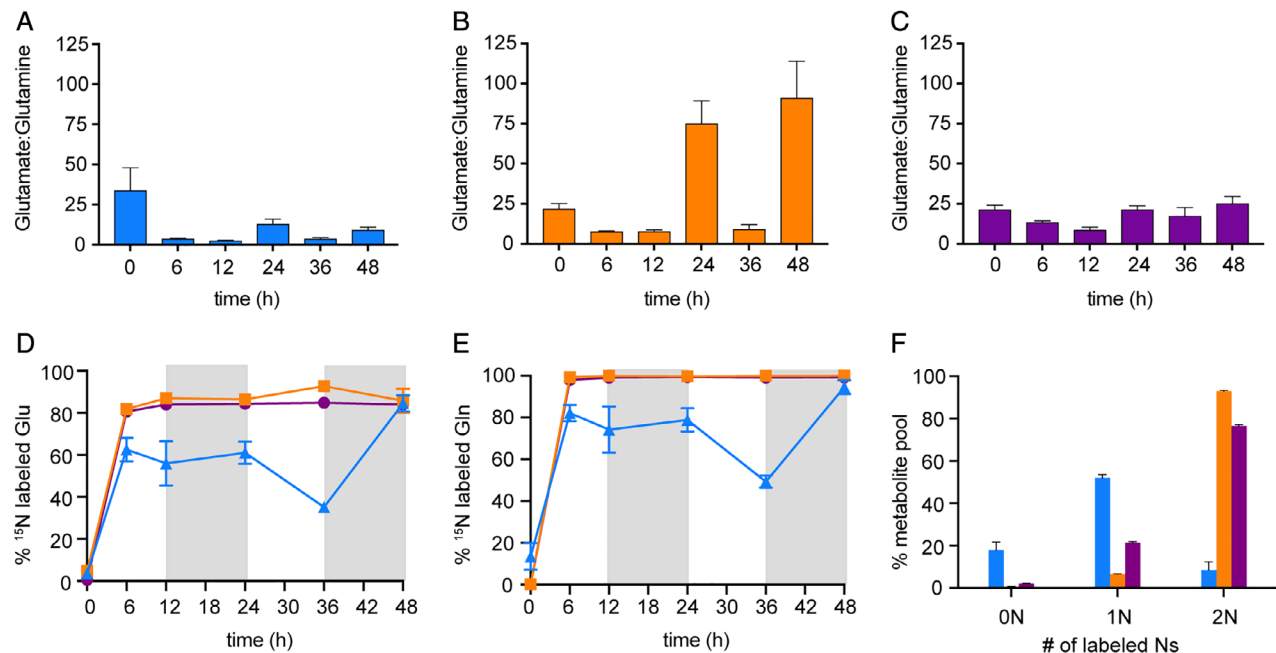


**Fig. 2.** Glutamate (GLU) and glutamine (GLN) dynamics in cells grown on  $\text{NO}_3$  (blue triangles),  $\text{NH}_4$  (orange squares), and urea (purple circles). A–C. Trends in GLU/GLN ratios are shown for  $\text{NO}_3$ ,  $\text{NH}_4$  and urea, respectively. D and E. The percentages GLU and GLN pool that has at least one N labelled with  $^{15}\text{N}$ , respectively. F. The percentage of differentially labelled Ns in GLN at  $T_6$ . The shading represents time points that were collected during the dark cycle. Error bars represent standard error.

labelled with 2Ns (~90%) compared to urea (~75%), and in  $\text{NO}_3^-$ , GLN pools only ever had 1 N labelled (Supporting Information Fig S2A-C).

Other metabolites in amino sugar metabolism and nucleoside synthesis pathways were labelled by all N species by  $T_{48}$ , such as UDP-N-acetylglucosamine, UDP-glucose and ADP/dGMP (Fig. 3A-C). The glutathione disulfide (GSSG) pool was also heavily labelled by all N species by  $T_{48}$  (Fig. 3D). Despite the flux of  $^{15}\text{N}$  into these core pathways, there were different trends in the number of labelled Ns per metabolite; the highest percentage for

the UDP-glucose and the downstream metabolite pool of UDP-N-acetylglucosamine at  $T_6$  was observed in cells grown on  $\text{NH}_4^+$  followed by urea. The AMP/dGMP and GSSG pools were more enriched in  $^{15}\text{N}$  when cells were grown on  $\text{NH}_4^+$  relative to the other N species (Fig. 3E-H). The labelling trends remained different across time as well (Supporting Information Fig. S2D-L), with  $\text{NH}_4^+$  saturating pools with a greater number of labelled Ns for all metabolites by  $T_{48}$ . Other labelled metabolites in amino sugar metabolism, primarily within the pyrimidine biosynthesis pathways, were detectable almost only in cells

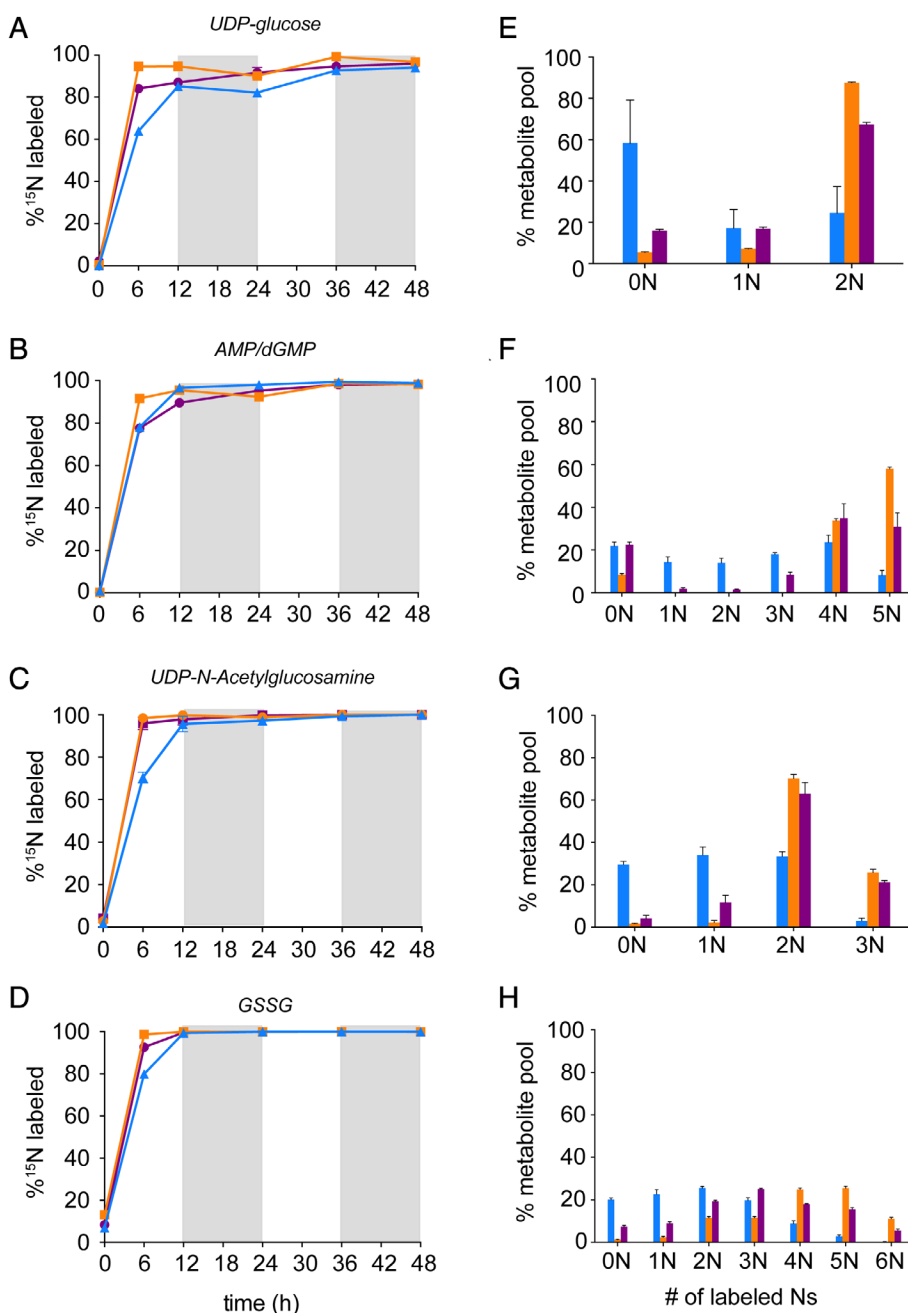


**Fig. 3.** Metabolites with  $^{15}\text{N}$  label across in N treatments; blue triangles =  $\text{NO}_3^-$ , orange squares =  $\text{NH}_4^+$ , purple circles = urea. A-D. Percent  $^{15}\text{N}$  represents the percentage of metabolites with at least one N labelled. Shading represents time points that were collected during the dark cycle. E-H. The percent of metabolites with different number of Ns labelled after 6 h for each metabolite in panel A–D. GSSG = Glutathionedisulfide. Error bars represent standard error.

grown on urea: most were not detectable in cells on  $\text{NO}_3$  and  $\text{NH}_4$  (Supporting Information Fig. S3). There were also several labelled amino acids observed in cells grown on urea (Supporting Information Fig. S4), corresponding to very few amino acids being detectable in cells grown on  $\text{NH}_4$  and  $\text{NO}_3$  in general (Supporting Information Fig. S5A and B). Abundances of many amino acids showed a diel pattern, increasing throughout the day and decreasing at night, especially on urea (Supporting Information Fig. S5C and Table S4), and this was not consistent across N species.

The arginine biosynthesis pathway was also enriched in  $^{15}\text{N}$  from urea. Key metabolites for arginine biosynthesis were detectable and over 80% labelled with  $^{15}\text{N}$  after only  $T_6$  (Fig. 4, Supporting Information Fig. S6). This labelling pattern was maintained through  $T_{48}$ . Fluctuations in abundances of metabolic intermediates within this pathway were observed (Supporting Information

Fig. S7 and Table S5): N-acetylglutamate and L-argininosuccinate accumulated overtime until  $T_{24}$  when they remained steady until  $T_{48}$ . This corresponded to a decrease in aspartate and citrulline, and an increase in arginine. Over 60% of the total citrulline ( $\text{Ns} = 3$ ) and ornithine ( $\text{Ns} = 2$ ) pools were completely labelled, whereas arginine and L-argininosuccinate ( $\text{Ns} = 4$ ) had a maximum of 3Ns labelled and 2Ns respectively.  $^{15}\text{N}$  from  $\text{NO}_3$  was detectable in only some pathway components: citrulline, aspartate, and N-acetylglutamate (Fig. 4A and Supporting Information Fig. S6). Arginine was detectable at very low levels in cells grown on  $\text{NO}_3$  (Supporting Information Dataset S1) but had no  $^{15}\text{N}$  signature (Fig. 4A and Supporting Information Fig. S7). Coupling between the GS-GOGAT cycle and arginine biosynthesis was evident in *M. aeruginosa* growing on  $\text{NO}_3$  in particular; these metabolites were labelled in a trend similar to GLU and GLN (Fig. 2 and Supporting Information Fig. S6).

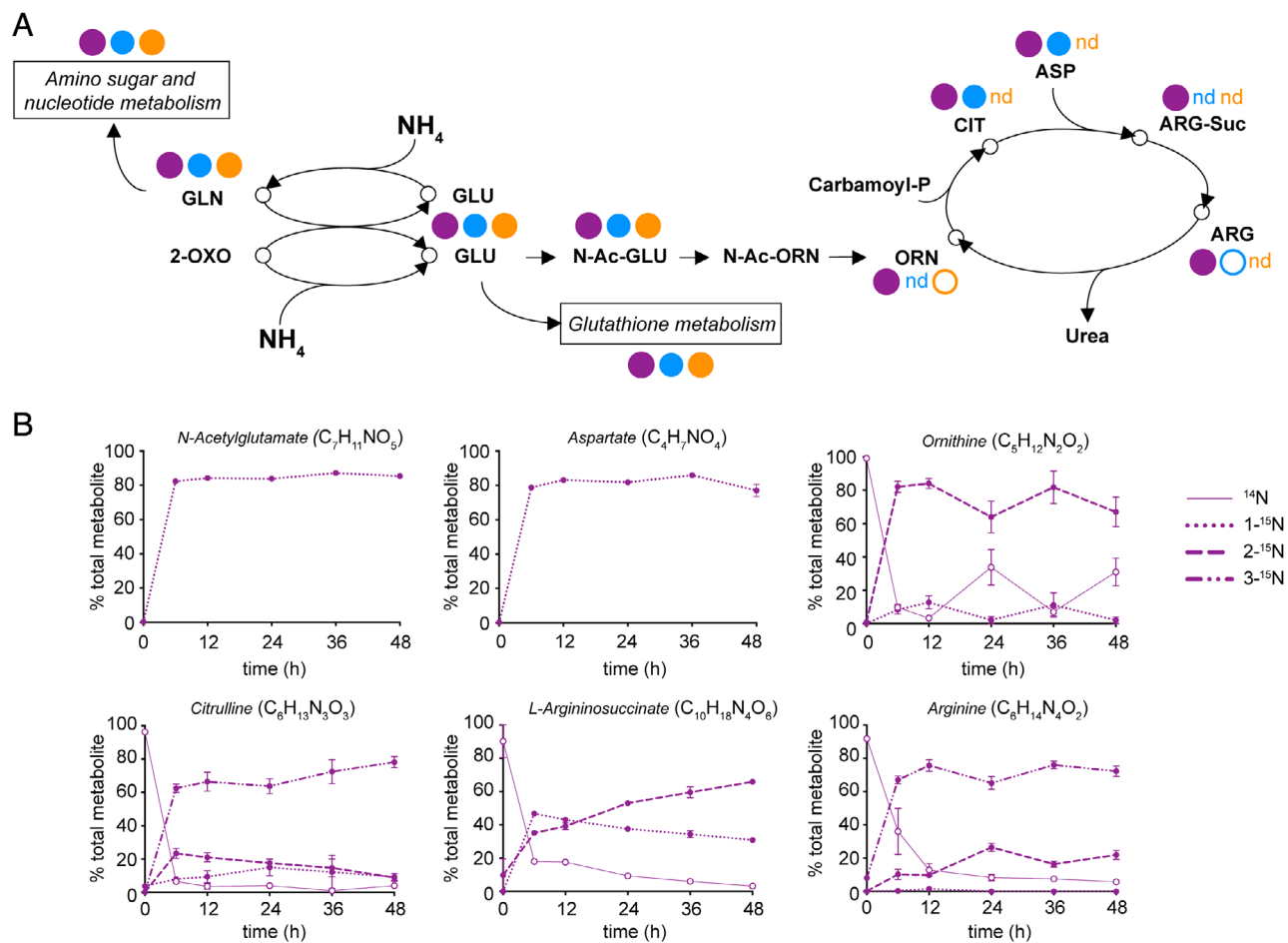


**Fig. 4.**  $^{15}\text{N}$  flux into the arginine biosynthesis pathway and the urea cycle from  $\text{NO}_3$  (blue),  $\text{NH}_4$  (orange) and urea (purple). A. Trends observed for  $^{15}\text{N}$  incorporation into the arginine biosynthesis pathway and urea cycle from all N species that were maintained at all time points following the addition of  $^{15}\text{N}$ . Closed symbols above a metabolite indicate  $^{15}\text{N}$  label was detectable, open circles indicate the metabolite was detectable but with no label, and 'nd' indicates no isotope of the metabolite was detected. B.  $^{15}\text{N}$  incorporation showing the percentage of Ns labelled in each metabolite from urea overtime. Error bars represent standard error.

N-acetylglutamate accumulated during the experiment, and while fluctuations in citrulline and aspartate were observed, arginine abundances did not ever increase (Supporting Information Fig. S7). The labelling dynamics of citrulline were distinct from those on urea; only ~40% of the pool was labelled and with mostly 2Ns until  $T_{48}$  (Supporting Information Fig. S8).  $^{15}\text{N}$  from  $\text{NH}_4$  was not detectable in any of the metabolites in these pathways except for N-acetylglutamate, although unlabelled ornithine was detectable at very low levels (Fig. 4A and Supporting Information Dataset S1).

#### Effect of N speciation on MC dynamics

Table S7 Differences in total MC quotas at  $T_0$  between N treatments were only weakly significant ( $p = 0.0697$ ), and

these differences were only observed between urea and  $\text{NO}_3$  ( $P = 0.0627$ ) and not  $\text{NH}_4$  and urea ( $P=0.736$ ) or  $\text{NO}_3$  and  $\text{NH}_4$  ( $P= 0.2626$ ; Fig. 5A and B, Supporting Information Table S7). There was a higher proportion of MC-FR in cells grown on urea and  $\text{NH}_4$ , MC-LR on  $\text{NO}_3$  and MC-dLR on urea, although the differences between urea and  $\text{NO}_3$  were only weakly significant. There were also weakly significant differences in MC-RR between  $\text{NH}_4$  and urea, while the relative abundances of MC-YR and MC-mLR were not different.

Incorporation of  $^{15}\text{N}$  into MC-LR and MC-RR increased with time in all N treatments (Fig. 5C). The proportion of MC-LR molecules labelled from urea increased more rapidly than  $\text{NO}_3$  and  $\text{NH}_4$ ; by  $T_{12}$  ~60% of the MC-LR pool was labelled with  $^{15}\text{N}$ .  $^{15}\text{N}$ -labelled MC-LR continued to increase during the two dark cycles (Supporting

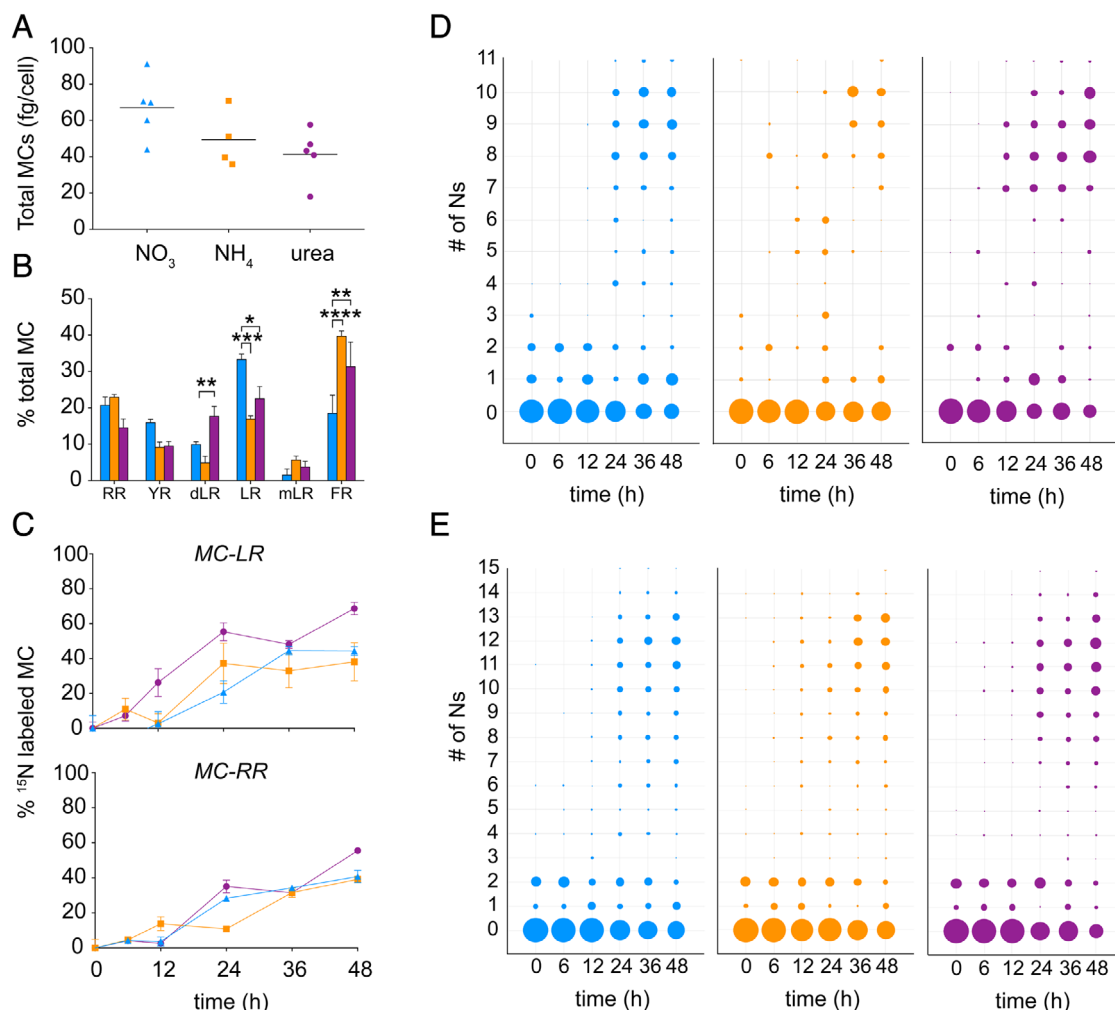


**Fig. 5.** Concentration, congener composition and flux of N into microcystins. A. Microcystin quotas (total MC concentrations per cell) at  $T_0$ . B. Congener composition at  $T_0$  in cells grown on  $\text{NO}_3$  (blue triangles),  $\text{NH}_4$  (orange squares), and urea (purple circles). C. The percentage of the MC-LR and MC-RR pool labelled with at least one  $^{15}\text{N}$  overtime in cells grown on  $\text{NO}_3$  (blue triangles),  $\text{NH}_4$  (orange squares), and urea (purple circles). D. Incorporation trends of  $^{15}\text{N}$  into MC-LR and MC-RR over time, respectively. The size of the symbols represent the proportion of MC-LR or MC-RR molecules labelled with that number of Ns at a certain time point; the larger the symbol, the greater the proportion. Error bars represent standard error.  $P$  values are reported using asterisks: \* =  $<0.05$ , \*\* =  $<0.01$ , \*\*\* =  $<0.001$  \*\*\*\*  $<0.0001$ .

Information Table S8). Increases in  $^{15}\text{N}$ -labelled MC-LR were not observed in cells grown on  $\text{NO}_3$  until the second light cycle, and despite a general increase over time in  $^{15}\text{N}$ -labelled MC-LR from  $\text{NH}_4$ , these increases were weakly significant. N flux from urea to MC-LR corresponded to increases in total MC-LR by  $T_{24}$ , but increased MC-LR abundances were not observed in cells grown on  $\text{NO}_3$  and  $\text{NH}_4$  (Supporting Information Fig. S9 and Table S9). The proportion of MC-RR labelled by  $\text{NH}_4$  increased during the light cycles, and  $^{15}\text{N}$ -labelled MC-RR increased on  $\text{NO}_3$  and urea during the dark cycle (Supporting Information Table S8), the latter only consistent in cells grown on urea. The trends in the proportional labelling of MC-LR and MC-RR pools corresponded to increases in the number of labelled Ns per molecule across time (Fig. 5D and E).

## Discussion

In this study,  $^{15}\text{N}$ -urea,  $^{15}\text{NO}_3$ , and  $^{15}\text{NH}_4$  were traced through the metabolome of a toxin-producing *M. aeruginosa* isolate to examine the specific physiological effects of N-chemistry on a bloom-forming cyanobacterium and to identify how it relates to the production of MCs. Using axenic cultures and labelled isotopes, it was confirmed that  $\text{NO}_3$ ,  $\text{NH}_4$  and urea were assimilated into cell metabolism (within 6 h) and could each be used as a sole N source to support growth of *M. aeruginosa*. Decreasing GLU:GLN, indicative that cells had become N-replete, on all N species during the day indicated that *M. aeruginosa* assimilated N when cells were photosynthesizing, suggesting N assimilation was coupled to C assimilation. Trends in total metabolite pools differed between light and dark samples, highlighting that the combined effects of C and N assimilation were linked to global metabolic shifts. Interestingly, metabolic trends due to diel cycling also differed depending on the available N species. This indicated that assimilation of different N species induced physiological changes in the light that also influenced the flux of N during the dark cycle.

Despite a similar overall trend, GLU:GLN were not driven by similar patterns in GLU and GLN abundances in N treatments. GLU and GLN are a main entry point for assimilated N after transport into the cell, and as a part of the GS-GOGAT (glutamine synthase-glutamate synthase) cycle, requires that all species of N are converted to  $\text{NH}_4$  prior to assimilation (Muro-Pastor *et al.*, 2005). For  $\text{NO}_3$ , this occurs through the  $\text{NO}_3$ -reductase pathway in a two-step process, first being converted to nitrite before  $\text{NH}_4$  (Flores and Herrero, 2005). Urea is hydrolyzed by the enzyme urease, which generates 1 mole each of  $\text{NH}_4$  and carbamate, the latter which should spontaneously dissociate to produce another mole of  $\text{NH}_4$  and carbon dioxide (Glibert *et al.*, 2016).

When  $\text{NH}_4$  is low, cells activate machinery for uptake and assimilation of  $\text{NO}_3$  and urea, although in many cyanobacteria urease is constitutive. The labeling of the GLN pools and other core metabolites suggested flux of N was faster in  $\text{NH}_4$  and urea than in cells grown on  $\text{NO}_3$ . Because these values are relative, it is possible that the pools of GLN in cells grown on  $\text{NH}_4$  and urea were smaller than those on  $\text{NO}_3$ , and therefore it would have taken less time to label multiple Ns compared to N treatments with larger pools of GLN. However, this would still indicate faster turnover of these metabolites and is consistent with the literature describing  $\text{NH}_4$  and urea as preferred N sources (Glibert *et al.*, 2016; Erratt *et al.*, 2018).  $\text{NH}_4$  is energetically less expensive to use than  $\text{NO}_3$ , and urea is considered more favourable than  $\text{NO}_3$  and  $\text{NH}_4$ , because assimilation of N requires less ATP and urea can readily be used a C source (Krausfeldt *et al.*, 2019). Examining flux at shorter intervals would be necessary to confirm this, but these data highlight that the regulation and energy expense involved in the assimilation of different N species led to changes in the flux of N through many downstream pathways.

Specific metabolic pathways that were influenced by N speciation were the amino acid, nucleotide, and amino sugar biosynthesis pathways, especially when urea was the sole N source. While the pools of several core metabolites involved in amino sugar and nucleoside biosynthesis were heavily labelled by only 6 h regardless of the N source, many more downstream metabolites in these pathways were labelled in only cells grown on urea. There was also incorporation of  $^{15}\text{N}$  into several amino acids in cells grown on urea that were not detectable with or without labelling in cells grown on  $\text{NO}_3$  and  $\text{NH}_4$ . Rapid flux into amino acid pathways and the production of N-rich compounds has been observed in other cyanobacteria with pulses of N after N starvation (Van de Waal *et al.*, 2010; Zhang *et al.*, 2018). However, GLU:GLN ratios did not support differences in the N status of the cell at  $T_0$  to indicate these observations were a factor of greater N limitation prior to  $^{15}\text{N}$  additions. Instead, this suggested that cells grown on urea were able to overcome some rate limiting step(s) to produce these metabolites. It is well established that C and N assimilation in cyanobacteria are linked (Tandeau de Marsac *et al.*, 2001, Muro-Pastor *et al.*, 2005). The diel fluctuations in many amino acid pools in cells grown on urea supported this, while also pointing again to the importance of urea as a C source since the same trends were not consistent on  $\text{NO}_3$  or  $\text{NH}_4$ . Purine and pyrimidine biosynthesis in  $\text{NO}_3$  and  $\text{NH}_4$  was potentially limited by C as well requiring a substantial amount of ATP and dependent on the production of 5-phosphoribosyl-1-pyrophosphate (PRPP) or activated ribose 5-phosphate (Hove-Jensen *et al.*, 2017), a product of the pentose phosphate pathway, to

produce downstream metabolites only detectable and labelled in urea. There were also two specific points where arginine biosynthesis appeared to be interrupted, both requiring ATP and reducing power for downstream reactions (Shin and Lee, 2014) in the  $\text{NH}_4$  and  $\text{NO}_3$  treatments: after the formation of N-acetylglutamate and the formation of aspartate and citrulline respectively.

These observations suggested that growth on urea led to greater production of ATP, reducing power and C cycling intermediates important for the assimilation of N and production of these essential metabolites. Indeed, previous studies have shown that growth on urea compared to  $\text{NO}_3$  and  $\text{NH}_4$  yielded greater photosynthetic efficiency (Erratt *et al.*, 2018). C limitation may explain the differences between  $\text{NO}_3$  and  $\text{NH}_4$  cultures, although the cultures were inverted at least once per day, caps were left loosened to allow gas exchange, and a previous study did not find transcriptomic evidence for C-limitation (Krausfeldt *et al.*, 2019). C or energy limitation does not clearly support the different patterns in labelling between  $\text{NH}_4$  and  $\text{NO}_3$ , since traditionally  $\text{NH}_4$  is considered more energetically efficient. This could indicate ammonia ( $\text{NH}_3$ ) toxicity, explaining the decreased fluorescence in these cultures compared to  $\text{NO}_3$  and urea;  $\text{NH}_3$  toxicity is related to PSII damage and decreased photosynthetic efficiency in other cyanobacteria (Drath *et al.*, 2008). However, photosynthetic efficiency can be higher on  $\text{NO}_3$  depending on the concentration of N supplied (Erratt *et al.*, 2018). Alternatively, cells grown on  $\text{NH}_4$  and  $\text{NO}_3$  may be expending energy on other essential functions, such as cell wall, lipid, or protein synthesis.

The enrichment of  $^{15}\text{N}$  in the arginine biosynthesis pathway could also indicate that cells grown on urea were shuttling more N into storage despite being provided at the same molar concentration as  $\text{NO}_3$  and  $\text{NH}_4$ . The arginine biosynthesis pathway includes the urea cycle, which is a route for removal of excess N in the form of urea in animals (Cunin *et al.*, 1986), but the absence of labelled urea indicates *M. aeruginosa* is not using it for this purpose. In addition to proteins, arginine is a key component of the N-storage molecule, cyanophycin. Cyanophycin is comprised of aspartate and arginine and produced by cyanobacteria in N-replete conditions (Shively, 2006; Llacer *et al.*, 2008; Maheswaran *et al.*, 2006), and the urea cycle itself (also termed the ornithine-arginine cycle) was proposed as important for N storage and cycling in *Synechocystis* (Zhang *et al.*, 2018). Abundances of L-argininosuccinate confirmed large fluxes of N into this pathway, indicating a potentially rate-limiting step in the production of arginine in cells grown on urea or supporting this cycle is used as N or C storage, as the cleavage of L-argininosuccinate yields fumarate along with arginine. Many enzymes within this pathway are negatively regulated by arginine,

and an increase in arginine by  $\text{T}_{24}$  and the accumulation of several preceding metabolites until arginine abundances decreased again, supported this regulation (Thompson, 1980; Shin and Lee, 2014). This could have been the cause for the lack of detection of many arginine biosynthetic intermediates in cells grown on  $\text{NO}_3$  and  $\text{NH}_4$ . Alternatively, arginine in cells grown on  $\text{NO}_3$  may be shuttled more rapidly into cyanophycin for storage thus preventing detection, whereas cells grown on urea may be accumulating more of these N-rich intermediate metabolites. The absence or low abundances of arginine pointed to limitations in its synthesis rather than rapid turnover, however, highlights the possibility that these N species are sensed differently by the cells.

Interestingly, labelling patterns did not support that the majority of arginine was made from L-argininosuccinate in cells grown on urea as would be expected from the classic biosynthesis pathway (Shin and Lee, 2014); L-argininosuccinate never had more than 2Ns labelled, whereas the majority of the arginine had 3Ns labelled through the whole experiment. Instead, it is possible that most of the arginine was made directly from citrulline, which also had 3Ns labelled through the whole 48 h; however, a BLAST search yielded no homologues for enzymes responsible for this reaction in *M. aeruginosa*. This could indicate an alternative route for arginine biosynthesis in *M. aeruginosa*. The saturation of  $^{15}\text{N}$  in the majority of the citrulline pool in cells grown on urea supports that there is flux of N into this pathway from carbamoyl-P. This is also evident in the  $\text{NO}_3$  treatment since no labelled ornithine was detectable. This supported growth on urea may increase flux from carbamoyl-P potentially due to the phosphorylation of the intermediate in urea hydrolysis, carbamate, which would increase flux of both C and N in to this cycle (Krausfeldt *et al.*, 2019).

These metabolic differences driven by N speciation corresponded to differences in MC dynamics. MCs are most well known as hepatotoxins that irreversibly bind to inhibit protein phosphatases, but they are also tumour promoters, endocrine disruptors, immunotoxins and irritants (Eriksson *et al.*, 1990; Codd *et al.*, 2017). Thus far, there have been over 200 different MC congeners identified that vary in their level of toxicity to mammals (Stoner *et al.*, 1989; Ikehara, *et al.*, 2009; Carmichael and Boyer, 2016). Although total MC concentrations at  $\text{T}_0$  were not different, the congener composition was different across N treatment. In this study, *M. aeruginosa* produced six N-rich congeners; MC-RR, -LR, YR, -FR, -dLR, and -mLR. The most toxic MC congener produced in this study was MC-LR, indicating that cells grown on  $\text{NO}_3$  and urea at  $\text{T}_0$  may have been more toxic to humans and animals than cells grown on  $\text{NH}_4$  despite similar MC quotas. However, the possibility for synergistic

effects cannot be discounted (Ibelings and Havens, 2008). Another congener which was prevalent in all N treatments was MC-FR, which is less toxic than MC-RR. This congener was not detected in previous studies using this strain such as in the study by Peng *et al.* (2018). Although culture conditions were similar, a major difference was the use of non-axenic cultures versus axenic in the current study. This would suggest interactions with heterotrophic bacteria alter MC congener composition and levels of toxicity per cell, adding another layer of complexity to studying MC dynamics in nature.

<sup>15</sup>N-labelling into MC-LR and MC-RR confirmed that cells were making MC on all N treatments and that the production of congeners varied due to N speciation. After the addition of new N, cells grown on urea turned over MC-LR at a faster rate than when NO<sub>3</sub> and NH<sub>4</sub> were the N source, and this corresponded to an increase in MC-LR abundances. Interestingly, MC-RR was turned over at a faster rate in cells grown on NH<sub>4</sub> during the light cycle, but NO<sub>3</sub> and urea matched in the proportion of labelled MC-RR during the first dark cycle. Clear, albeit opposite, diel patterns were observed for urea and NH<sub>4</sub> that were not maintained in cells grown on NO<sub>3</sub> or for MC-LR on any N species. These results indicated that MC congener composition and concentrations were not static, and *M. aeruginosa* did not produce MC or individual congeners uniformly. Further, these data suggest that cells grown on urea were turning over and producing more MCs than when grown on NO<sub>3</sub> and NH<sub>4</sub>, which has important implications in lakes and other water bodies that are heavily impacted by agriculture.

The labelling dynamics observed in MC-LR and MC-RR for urea may be linked to the higher flux of urea-N into amino acids, especially those that are precursors for MC. Indeed, the addition of some amino acids, like arginine, alanine and leucine, to media has supported MC synthesis in *Microcystis* spp. (Dai *et al.*, 2009), and intracellular amino acid availability has been linked to both cyanophycin and MC production in *Planktothrix*, another toxic bloom forming cyanobacteria (Van de Waal *et al.*, 2010). The specific addition of arginine seems to be important, and it was discovered to be the last amino acid added to the MC molecule (Dai *et al.*, 2019). Therefore, this study supports that there is likely a link between MC and arginine production, and the production of arginine itself may be a limiting step in the synthesis of MC. The different incorporation trends between MC-LR and MC-RR could indicate that the production of congeners was not strictly related to substrate availability. Congener composition has been linked to N availability with high N leading to more N-rich MC congeners, like MC-RR (Tonk *et al.*, 2008; Van de Waal *et al.*, 2009, 2010; Puddick *et al.*, 2016). In this study, where the molar concentration of N was equivalent, the concentrations of MC-RR were not

different at T<sub>0</sub> but did differ in less N-rich congeners. The differences in the trends of amino acids and MC production and turnover on urea could also be a factor of 2 moles of NH<sub>4</sub> being produced per 1 mole of urea allowing for saturation of N-rich metabolites an ability to overcome C or energy limitations that cells growing on NH<sub>4</sub> and NO<sub>3</sub> cannot. Further insight to this is needed since many of these amino acids were only detectable on urea and MCs were produced on all N species, but these data indicate congener composition is not strictly a factor of N availability.

Despite decades of research, the underlying function of MCs in cyanobacteria is still not clear, and its production has been linked to several factors and many functions have been proposed (Neilan *et al.*, 2013; Gobler *et al.*, 2016; Harke *et al.*, 2016). Other factors in addition to N have been examined influencing MC production, including P concentrations, C availability, light levels, temperature, and trace metal availability (Neilan *et al.*, 2013), and results are often conflicting or difficult to separate from the influence of growth rate. Here, *M. aeruginosa* was grown under the same incubation conditions, molar N concentrations that maintained a similar generation time, and cultured axenically to remove these confounding factors. Thus, the specific influence of N speciation on MC production can be determined. These data support that it does impact MC congener composition, the level of toxicity, the turnover and the production of MCs, and influence of N speciation on MCs in the environmental are not just a factor of community composition shifts. It is important to note that the physiological differences observed here are true for this set of conditions, which had consistent light levels, the same incubation conditions and media components (with the exception of N species) and were grown axenically in batch culture. This is not necessarily representative of what occurs in the environment. The metabolic shifts driven by differences in N flux could vary with factors that influence N uptake or enzyme efficiency, such as C availability, temperature, pH and competition with bloom associated bacteria. Yet to address the importance of N speciation and N as a whole on the metabolism of *Microcystis* and MC production, a controlled system with a single organism is an essential first step. Extrapolating this and similar approaches to field conditions should result in a better characterization of the complicated interacting factors that drive *Microcystis* bloom formation and toxin production.

## Experimental procedures

### Culture conditions and <sup>15</sup>N incorporation

Stock cultures of axenic *Microcystis aeruginosa* NIES-843, isolated from Lake Kasumigaura Ibaraki Japan (Otsuka *et al.*, 2000, 2001), were maintained and continuously transferred in 25 ml of modified CT medium (briefly,

0.05 g  $\text{Na}_2\text{B}$ -glycerophosphate, 0.04 g  $\text{MgSO}_4 \cdot 7\text{H}_2\text{O}$ , and trace metals, buffered with 0.2 g TAPS; Steffen *et al.*, 2014); at a pH of 8.2 ( $\pm 0.05$ ) with 0.595 mM N ( $\text{NO}_3$  provided as  $\text{KNO}_3/\text{CaNO}_3 \cdot 4\text{H}_2\text{O}$ ,  $\text{NH}_4$  provided as  $\text{NH}_4\text{Cl}$ , or urea) in 50 ml screw cap glass culture tubes. The cultures were incubated without shaking at 26°C on a diel cycle (12:12 h) within the range of 50–60  $\mu\text{mol}$  photon  $\text{m}^{-2} \text{s}^{-1}$  of light. Culture tubes were inverted three times daily, and caps were loosened to allow for gas exchange. Microbial contamination checks were performed regularly by microscopy as well as for heterotrophic microbial growth in purity tubes of both rich and minimal media (LB medium and CT medium +0.05% glucose, 0.05% acetate, 0.05% pyruvate and 0.05% lactate, respectively). Cell concentrations were measured using flow cytometry (Guava easyCyte HT, Millipore) and chlorophyll a autofluorescence (fluorescence signal units, FSU) was measured using a fluorometer (Turner Designs TD-700), over the course of the experiment.

Prior to  $^{15}\text{N}$  additions, axenic *M. aeruginosa* cultures were acclimated to experimental concentrations with their respective  $^{14}\text{N}$  sources for at least three transfers. For the  $^{15}\text{N}$ -incorporation experiment, acclimated cells were grown on  $^{14}\text{N}$  in 10  $\times$  50 ml culture tubes with 25 ml of media. When the cells reached mid-log phase ( $\sim 300\ 000$ – $400\ 000$  cell  $\text{mL}^{-1}$ ), they were filter concentrated on 1.0- $\mu\text{m}$  polycarbonate filters and resuspended in one 50 ml culture tube with 30 ml of fresh  $^{14}\text{N}$  media. This occurred approximately 24 h prior to the start of the experiment to maintain logarithmic growth. Cells were checked for contamination and transferred to  $^{15}\text{N}$  media ( $> 98\%$   $^{15}\text{N}$  saturated  $\text{NH}_4\text{Cl}$ , urea, or  $\text{KNO}_3/\text{Ca}(\text{NO}_3)_2$ ), with a starting concentration of  $\sim 1.15 \times 10^5$  cells  $\text{mL}^{-1}$  to reach a final volume of 25 ml in 50 ml culture tubes (Supporting Information Table S1). Twenty-five tubes were prepared per treatment to be randomly harvested at 6, 12, 24, 36, and 48 h (with five replicates at each time point) after inoculation at the start of the day cycle. The 12 h and 36 h time points were collected immediately before the next dark cycle, and the 24 h and 48 h time points were collected immediately before the next light cycle. Five tubes were prepped with 25 ml of  $^{14}\text{N}$  media per treatment and inoculated at the same starting concentration to serve as time 0 (no  $^{15}\text{N}$  addition) control. FSU was measured, and cell counts were collected for all tubes at time 0. At each time point, five tubes were randomly picked, FSU was measured and  $2 \times 200 \mu\text{l}$  were collected for replicate cell counts. The remaining 24.6 ml of culture in each tube were harvested by filtration on a 1.0  $\mu\text{m}$  polycarbonate filter. The filter was immediately flash frozen in 2 ml cryovials using liquid N and stored at  $-80^\circ\text{C}$  until extraction of metabolites. Samples that were lost in the experiment or did not grow and were excluded from the analysis can be found in the

Supporting Information Table S1. Metabolites were extracted and processed as previously described (Krausfeldt *et al.*, 2019).

#### *Microcystin quantification and incorporation*

Intracellular MC concentrations were determined without preconcentration using HPLC coupled with single quadrupole mass spectroscopy and photodiodearray spectroscopy as described by Tang *et al.* (2018). Standards (MC-RR, -LR and -LF) were run at the start and end of each run to ensure that the retention times for the MCs did not drift, and individual toxin congeners [(RR, dRR, mRR, hYR, YR, LR, mL, zLR, dLR, meLR, AR, FR, WR, LA, LY, LW, LF, WR) and R-NOD] were identified on the basis of their retention time, their characteristic absorbance spectrum in the photodiode array detector and their characteristic molecular ions. Samples were analysed both in centroid and continuum mode. These data were used to analyse differences in congener composition in all N treatments.

To determine the  $^{15}\text{N}$  incorporation into MC-LR and MC-RR, the above HPLC method was coupled with a tandem mass spectrometer. MC-LR ( $\text{C}_{49}\text{H}_{74}\text{N}_{10}\text{O}_{12}$ ) transitions from the protonated molecular ion to the *m/z* 135 ADDA fragment were set up in 1 amu intervals up to twelve  $^{15}\text{N}$  being incorporated [e.g. *m/z* 995.6  $\rightarrow$  135.1 (no  $^{15}\text{N}$ , *m/z* 996.6  $\rightarrow$  135.1 (one  $^{15}\text{N}$ ), 997.5  $\rightarrow$  135.1 (two  $^{15}\text{N}$ )...*m/z* 1006.6  $\rightarrow$  135.1 (twelve  $^{15}\text{N}$ )]. MC-RR ( $\text{C}_{49}\text{H}_{75}\text{N}_{13}\text{O}_{12}$ ) transitions were examined using the diprotонated molecular ion in half mass unit intervals [e.g. *m/z* 519.7  $\rightarrow$  135.1 (no  $^{15}\text{N}$ ), *m/z* 520.2 (one  $^{15}\text{N}$ ), 520.7  $\rightarrow$  135.1 (three  $^{15}\text{N}$ )] up to the incorporation of sixteen  $^{15}\text{N}$  into MC-RR. MRM tuning and fragmentation parameters for the MRM analysis were derived using non-labelled MC-LR and -RR standards obtained from Abraxas. Peak areas were normalized to exclude natural  $^{13}\text{C}$  abundances in MC-LR and MC-RR for analyses of  $^{15}\text{N}$  incorporation overtime. The sum of all peak areas in a sample for labelled and unlabelled MC-LR was normalized by cell number used to calculate fold changes overtime with  $T_0$  serving as the baseline.

#### *Data analyses and statistics*

Doubling times were calculated manually using the cell concentrations at  $T_0$  and  $T_{48}$ . Relative metabolite abundances ('total' abundances) were calculated by adding the  $^{14}\text{N}$  and  $^{15}\text{N}$  peak areas and normalizing by cell concentration for each metabolite within each N treatment. A 3D non-metric multidimensional scaling (NMDS) analysis was performed in Primer-E v7 (Clarke and Gorley, 2006) using fold change differences compared to the average abundance of each metabolite at  $T_0$  for only the

23 metabolites detectable in every N treatment. This was done to eliminate any bias in the trends observed due to metabolites that were undetectable in some treatments (below the detection limit of the instrument). Samples were clustered by similarity using Pearson correlations calculated after a square root transformation of these values for each sample. One-way ANOSIM determined differences in metabolic trends due to N speciation and diel cycling. Pathways for metabolites with and without  $^{15}\text{N}$  signatures were determined using the Kyoto Encyclopedia of Genes and Genomes (KEGG) database. Percent incorporation was calculated by dividing  $^{15}\text{N}$  peak areas by sum of  $^{15}\text{N} + ^{14}\text{N}$  peak areas for each metabolite. Statistically significant differences between doubling times and fold changes abundances in metabolites were calculated using one-way ANOVA followed by Tukey's multiple comparisons test. Statistical significance was defined as having a  $P$  value  $<0.05$ . Weakly significant relationships were also reported and defined as having a  $P$  value between 0.05 and 0.10.

### Author contributions

L.K. and S.W. conceived the study. L.K. performed cultivation and the  $^{15}\text{N}$  experiments. L.K. extracted metabolites and A.F., H.C. and S.R. performed metabolomics. G.B. analysed the microcystin congeners and  $^{15}\text{N}$  incorporation into the microcystin-LR and microcystin-RR. All authors contributed to data analysis and manuscript preparation.

### Acknowledgements

The authors thank George Bullerjahn, R. Michael McKay, Gary LeCleir and Robbie Martin for discussions regarding this paper. This work was supported by grants from the National Science Foundation (DEB 1240870 to SWW; IOS 1451528 and DBI 1530975 to SWW and SRC), funding from the NIEHS (1P01ES028939-01) and NSF (OCE-1840715) to SWW through the *Great Lakes Center for Fresh Waters and Human Health*, and the *Kenneth and Blaire Mossman Endowment* to the University of Tennessee.

### References

Belisle, B.S., Steffen, M.M., Pound, H.L., Watson, S.B., DeBruyn, J.M., Bourbonnierre, R.A., et al. (2016) Urea in Lake Erie: organic nutrient sources as potentially important drivers of phytoplankton biomass. *JGLR* **42**: 599–607.

Beversdorf, L.J., Miller, T.R., and McMahon, K.D. (2015) Long-term monitoring reveals carbon–nitrogen metabolism key to microcystin production in eutrophic lakes. *Front Microbiol* **6**: 456.

Bullerjahn, G.S., McKay, R.M., Davis, T.W., Baker, D.B., Boyer, G.L., D'Anglada, L.V., et al. (2016) Global solutions to regional problems: collecting global expertise to address the problem of harmful cyanobacterial blooms. *A Lake Erie case study Harmful Algae* **54**: 223–238.

Carmichael, W.W., and Boyer, G.L. (2016) Health impacts from cyanobacteria harmful algae blooms: implications for the north American Great Lakes. *Harmful Algae* **54**: 194–212.

Chaffin, J.D., and Bridgeman, T.B. (2013) Organic and inorganic nitrogen utilization by nitrogen-stressed cyanobacteria during bloom conditions. *J Appl Phycol* **26**: 299–309.

Chaffin, J.D., Davis, T.W., Smith, D.J., Baer, M.M., and Dick, G. J. (2018) Interactions between nitrogen form, loading rate, and light intensity on *Microcystis* and *Planktothrix* growth and microcystin production. *Harmful Algae* **73**: 84–97.

Clarke, K., and Gorley, R. (2006) *PRIMER v6: User Manual/Tutorial (Plymouth Routines in Multivariate Ecological Research)*. Plymouth: Primer-E Ltd.

Codd, G. A., Fastner, J., Lindholm, T., Meriluoto, J., & Metcalf, J. S. (2017). Interpretation, Significance, and Reporting of Results. *Handbook of Cyanobacterial Monitoring and Cyanotoxin Analysis*, **292**.

Cunin, R., Glansdorff, N., Pierard, A., and Stalon, V. (1986) Biosynthesis and metabolism of arginine in bacteria. *Microbiol Rev* **50**: 314.

Dai, R., Liu, H., Qu, J., Zhao, X., and Hou, Y. (2009) Effects of amino acids on microcystin production of the *Microcystis aeruginosa*. *J Hazard Mater* **161**: 730–736.

Dai, R., Zhou, Y., Chen, Y., Zhang, X., Yan, Y., and An, D. (2019) Effects of arginine on the growth and microcystin-LR production of *Microcystis aeruginosa* in culture. *Sci Total Environ* **651**: 706–712.

Davis, T.W., Harke, M.J., Marcoval, M.A., Goleski, J., Oran-Dawson, C., Berry, D.L., and Gobler, C.J. (2010) Effects of nitrogenous compounds and phosphorus on the growth of toxic and non-toxic strains of *Microcystis* during cyanobacterial blooms. *Aquat Microb Ecol* **61**: 149–162.

Drath, M., Kloft, N., Batschauer, A., Marin, K., Novak, J., and Forchhammer, K. (2008) Ammonia triggers photodamage of photosystem II in the cyanobacterium *Synechocystis* sp. strain PCC 6803. *Plant Physiol* **147**: 206–215.

Erratt, K.J., Creed, I.F., and Trick, C.G. (2018) Comparative effects of ammonium, nitrate and urea on growth and photosynthetic efficiency of three bloom-forming cyanobacteria. *Freshwater Biol* **63**: 626–638.

Eriksson, J.E., Toivola, D., Meriluoto, J.A.O., Karaki, H., Han, Y.G., and Hartshorne, D. (1990) Hepatocyte deformation induced by cyanobacterial toxins reflects inhibition of protein phosphatases. *Biochem Biophys Res Comm* **173**: 1347–1353.

Flores, E., and Herrero, A. (2005) Nitrogen assimilation and nitrogen control in cyanobacteria. *Biochem Soc Trans* **33**: 164–167.

Flynn, K.J., Dickson, D.M., and Al-Amoudi, O.A. (1989) The ratio of glutamine: glutamate in microalgae: a biomarker for N-status suitable for use at natural cell densities. *J Plankton Res* **11**: 165–170.

Ginn, H., Pearson, L., and Neilan, B. (2010) NtcA from *Microcystis aeruginosa* PCC 7806 is autoregulatory and binds to the microcystin promoter. *Appl Environ Microbiol* **76**: 4362–4368.

Glibert, P.M., Harrison, J., Heil, C., and Seitzinger, S. (2006) Escalating worldwide use of urea—a global change

contributing to coastal eutrophication. *Biogeochemistry* **77**: 441–463.

Glibert, P.M., Maranger, R., Sobota, D.J., and Bouwman, L. (2014) The Haber Bosch–harmful algal bloom (HB–HAB) link. *Environ Res Let* **9**: 105001.

Glibert, P.M., Wilkerson, F.P., Dugdale, R.C., Raven, J.A., Dupont, C.L., Leavitt, P.R., et al. (2016) Pluses and minuses of ammonium and nitrate uptake and assimilation by phytoplankton and implications for productivity and community composition, with emphasis on nitrogen-enriched conditions. *Limnol Oceanogr* **61**: 165–197.

Gobler, C.J., Burkholder, J.M., Davis, T.W., Harke, M.J., Johengen, T., Stow, C.A., and Van de Waal, D.B. (2016) The dual role of nitrogen supply in controlling the growth and toxicity of cyanobacterial blooms. *Harmful Algae* **54**: 87–97.

Hampel, J.J., McCarthy, M.J., Neudeck, M., Bullerjahn, G.S., McKay, R.M.L., and Newell, S.E. (2019) Ammonium recycling supports toxic *Planktothrix* blooms in Sandusky Bay. *Lake Erie: Evidence from stable isotope and meta-transcriptome data* *Harmful Algae* **81**: 42–52.

Harke, M.J., and Gobler, C.J. (2015) Daily transcriptome changes reveal the role of nitrogen in controlling microcystin synthesis and nutrient transport in the toxic cyanobacterium *Microcystis aeruginosa*. *BMC Genomics* **16**: 1068.

Harke, M.J., Davis, T.W., Watson, S.B., and Gobler, C.J. (2015) Nutrient-controlled niche differentiation of western Lake Erie cyanobacterial populations revealed via meta-transcriptomic surveys. *Environ Sci Technol* **50**: 604–615.

Harke, M.J., Steffen, M.M., Gobler, C.J., Otten, T.G., Wilhelm, S.W., Wood, S.A., and Paerl, H.W. (2016) A review of the global ecology, genomics, and biogeography of the toxic cyanobacterium *Microcystis* spp. *Harmful Algae* **54**: 4–20.

Hove-Jensen, B., Andersen, K.R., Kilstrup, M., Martinussen, J., Switzer, R.L., and Willemoes, M. (2017) Phosphoribosyl diphosphate (PRPP): biosynthesis, enzymology, utilization, and metabolic significance. *Microbiol Mol Biol Rev* **81**: e00040–e00016.

Ibelings, B.W., and Havens, K.E. (2008) Cyanobacterial toxins: a qualitative meta-analysis of concentrations, dosage and effects in freshwater, estuarine and marine biota. In *Cyanobacterial Harmful Algal Blooms: State of the Science and Research Needs*. New York, NY: Springer, pp. 675–732.

Ikehara, T., Imamura, S., Sano, T., Nakashima, J., Kuniyoshi, K., Oshiro, N., et al. (2009) The effect of structural variation in 21 microcystins on their inhibition of PP2A and the effect of replacing cys<sup>269</sup> with glycine. *Toxicon* **54**: 539–544.

Krausfeldt, L.E., Farmer, A.T., Castro, G.H., Zepernick, B.N., Campagna, S.R., and Wilhelm, S.W. (2019) Urea is both a carbon and nitrogen source for *Microcystis aeruginosa*: tracking <sup>13</sup>C incorporation at bloom pH conditions. *Front Microbiol* **10**: 1064.

Llacer, J.L., Fita, I., and Rubio, V. (2008) Arginine and nitrogen storage. *Curr Op Struct Biol* **18**: 673–681.

Maheswaran, M., Ziegler, K., Lockau, W., Hagemann, M., and Forchhammer, K. (2006) PII-regulated arginine synthesis controls accumulation of cyanophycin in *Synechocystis* sp. strain PCC 6803. *J Bacteriol* **188**: 2730–2734.

Muro-Pastor, M.I., Reyes, J.C., and Florencio, F.J. (2005) Ammonium assimilation in cyanobacteria. *Photosynthesis Res* **83**: 135–150.

Neilan, B.A., Pearson, L.A., Muenchhoff, J., Moffitt, M.C., and Dittmann, E. (2013) Environmental conditions that influence toxin biosynthesis in cyanobacteria. *Environ Microbiol* **15**: 1239–1253.

Newell, S.E., Davis, T.W., Johengen, T.H., Gossiaux, D., Burtner, A., Palladino, D., and McCarthy, M.J. (2019) Reduced forms of nitrogen are a driver of non-nitrogen-fixing harmful cyanobacterial blooms and toxicity in Lake Erie. *Harmful Algae* **81**: 86–93.

Otsuka, S., Suda, S., Li, R., Matsumoto, S., and Watanabe, M.M. (2000) Morphological variability of colonies of *Microcystis* morphospecies in culture. *J Gen Appl Microbiol* **46**: 39–50.

Otsuka, S., Suda, S., Shibata, S., Oyaizu, H., Matsumoto, S., and Watanabe, M.M. (2001) A proposal for the unification of five species of the cyanobacterial genus *Microcystis* Kützing ex Lemmermann 1907 under the rules of the bacteriological code. *Int J Syst Evolut Microbiol* **51**: 873–879.

Paerl, H.W., Gardner, W.S., McCarthy, M.J., Peierls, B.L., and Wilhelm, S.W. (2014) Algal blooms: noteworthy nitrogen. *Science* **346**: 175.

Paerl, H.W., Scott, J.T., McCarthy, M.J., Newell, S.E., Gardner, W., Havens, K.E., et al. (2016) It takes two to tango: when and where dual nutrient (N and P) reductions are needed to protect lakes and downstream ecosystems. *Environ Sci Technol* **50**: 10805–10813.

Peng, G., Martin, R., Dearth, S., Sun, X., Boyer, G.L., Campagna, S., et al. (2018) Seasonally-relevant cool temperatures interact with N chemistry to increase microcystins produced in lab cultures of *Microcystis aeruginosa* NIES-843. *Environ Sci Technol* **52**: 4127–4136.

Puddick, J., Prinsep, M.R., Wood, S.A., Cary, S.C., and Hamilton, D.P. (2016) Modulation of microcystin congener abundance following nitrogen depletion of a *Microcystis* batch culture. *Aquat Ecol* **50**: 235–246.

Schindler, D.W. (1977) Evaluation of phosphorus limitation in lakes. *Science* **195**: 260–262.

Schindler, D.W., and Vallentyne, J.R. (2008) *The Algal Bowl: Overfertilization of the World's Freshwaters and Estuaries*. Edmonton, Alberta, Canada: University of Alberta Press.

Shin, J.H., and Lee, S.Y. (2014) Metabolic engineering of microorganisms for the production of L-arginine and its derivatives. *Microb Cell Fact* **13**: 166.

Shively, J.M. (2006) *Inclusions in Prokaryotes*. Heidelberg: Springer Science and Business Media.

Steffen, M.M., Dearth, S.P., Dill, B.D., Li, Z., Larsen, K.M., Campagna, S.R., and Wilhelm, S.W. (2014) Nutrients drive transcriptional changes that maintain metabolic homeostasis but alter genome architecture in *Microcystis*. *ISME J* **8**: 2080–2092.

Stoner, R.D., Adams, W.H., Slatkin, D.N., and Siegelman, H. W. (1989) The effects of single L-amino acid substitutions on the lethal potencies of the microcystins. *Toxicon* **27**: 825–828.

Tandeau de Marsac, N.T., Lee, H., Hisbergues, M., Castets, A., and Bédu, S. (2001) Control of nitrogen and carbon metabolism in cyanobacteria. *J Appl Phycol.* **13**: 287–292.

Tang, X., Krausfeldt, L. E., Shao, K., LeCleir, G. R., Stough, J. M., Gao, G., et al. (2018). Seasonal gene expression and the ecophysiological implications of toxic *Microcystis aeruginosa* blooms in Lake Taihu. *Environmental science & technology*, **52**(19): 11049–11059.

Thompson, J.F. (1980) Arginine synthesis, proline synthesis, and related processes. In *Amino Acids and Derivatives*. Cambridge, MA: Academic Press, pp. 375–402.

Tonk, L., Van De Waal, D.B., Slot, P., Huisman, J., Matthijs, H.C., and Visser, P.M. (2008) Amino acid availability determines the ratio of microcystin variants in the cyanobacterium *Planktothrix agardhii*. *FEMS Microbiol Ecol* **65**: 383–390.

Van de Waal, D.B., Verspagen, J.M., Lürling, M., Van Donk, E., Visser, P.M., and Huisman, J. (2009) The ecological stoichiometry of toxins produced by harmful cyanobacteria: an experimental test of the carbon-nutrient balance hypothesis. *Ecol Lett* **12**: 1326–1335.

Van de Waal, D.B., Ferreruela, G., Tonk, L., Van Donk, E., Huisman, J., Visser, P.M., and Matthijs, H.C. (2010) Pulsed nitrogen supply induces dynamic changes in the amino acid composition and microcystin production of the harmful cyanobacterium *Planktothrix agardhii*. *FEMS Microbiol Ecol* **74**: 430–438.

Wilhelm, S.W., DeBruyn, J.M., Gillor, O., Twiss, M.R., Livingston, K., Bourbonniere, R.A., et al. (2003) Effect of phosphorus amendments on present day plankton communities in pelagic Lake Erie. *Aquat Microb Ecol* **32**: 275–285.

Zhang, H., Liu, Y., Nie, X., Liu, L., Hua, Q., Zhao, G.P., and Yang, C. (2018) The cyanobacterial ornithine–ammonia cycle involves an arginine dihydrolase. *Nat Chem Biol* **1**: 575.

### Supporting Information

Additional Supporting Information may be found in the online version of this article at the publisher's web-site:

**Appendix S1:** Supporting Information